Hindawi
Complexity
Volume 2022, Article ID 4038598, 15 pages
https://doi.org/10.1155/2022/4038598

Research Article

Observer-Based Synchronization and Quasi-Synchronization for Multiple Neural Networks with Time-Varying Delays

Biwen Li, Donglun Wang, and Jingjing Huang

College of Mathematics and Statistics, Hubei Normal University, Huangshi 435002, China

Correspondence should be addressed to Biwen Li; lbw20200320@163.com

Received 28 March 2022; Revised 18 May 2022; Accepted 24 June 2022; Published 9 September 2022

Academic Editor: Miaomiao Wang

In this paper, we study the synchronization of a class of multiple neural networks (MNNs) with delay and directed disconnected switching topology based on state observer via impulsive coupling control. The coupling topology is connected sequentially, and the controller adjusts the state value through event-triggering strategies. Different from the related works on MNNs, its state in this paper is assumed to be unmeasurable, and the time delay is also unmeasurable. Therefore, the observer does not contain the time-delay term. The impulsive switching controller and observer controller adjust the system through the observed value. By constructing the corresponding augmented matrix, the system can finally achieve quasi-synchronization (synchronization). Through derivation, we give the sufficient conditions ensuring quasi-synchronization (synchronization) via the event-triggered impulse control mechanism. In addition, numerical simulation examples are given to test our results of the theorem.

1. Introduction

There has been rapid development of multi-agent systems (MASs). In practical application, the application of MAS mainly includes power engineering [1], bioengineering [2], robot formation control [3], vehicle formation control [4], and some other fields. Theoretically, the dynamic behavior of MAS, such as stability [5], robustness [6], synchronization [7], and so on, has become the basis of various theories and greatly promoted the development of MAS. So far, a number of achievements have been made in the study of MAS.

In addition, as a complex network, the topology of MAS plays an important role in the dynamic behavior. For example, in [8], second-order leaderless and leader-following consensus algorithms with communication and input delays in directed network topology are studied. In addition, this paper involves three different situations: leaderless consumption, consumption regulation, and consumption tracking. On the other hand, the network topology plays an important role in the asymptotical stability scheme. In the leader-following problem of multi-agent network, it is assumed that the network topology switches arbitrarily between limited topology sets and there is a time-varying delay in the coupling of agents [9]. Different from the general topology, the switching topology in this paper is of great significance to the sudden change or failure of the environment, so switching topology widely exists in MAS.

In recent years, MNNs have been widely used, especially in automatic control [10], signal processing [11], optimization [12], and so on. Such complex systems are extremely dependent on the synchronization and stability of MNNs. Therefore, synchronization problem is receiving more and more attention and has always been a very important research direction [13–16]. Especially, Chen et al. [16] considered synchronization for nonlinear neural complex networks by a switching topology. On the other hand, different from synchronous, quasi-synchronous is a special form of dynamical behavior, where all of the control systems in networks are almost synchronized with a given synchronization error, which could not tend to zero with time. Chen et al. [17] discussed the quasi-synchronization problem through a coupled memristor neural network with time-varying delay. The quasi-synchronization problem in fractional-order multi-layer networks with fractional mismatch is studied in [18].

With the development of industrial demand and information technology, some traditional control strategies have been replaced by other control schemes. The feasibility and advantages of event-triggered control (ETC) have been proposed for the first time since 1999. Different from traditional control scheme, ETC can ensure system performance while effectively reducing the execution of control tasks. In recent years, ETC has become a popular research subject [19–22]. Because we only need to adjust the state of the controller at the event-trigger instants via setting an appropriate event-trigger mechanism. Different from continuous control and ETC, controller status is updated only at the moment of event trigger, it is adjusted to meet the needs of the system. At present, existing work of ETC in the multiagent field (see [23, 24]). Especially, [25] the recurrent neural network triggered by finite-time event-triggered strategy is studied, and the stability of finite-time systems is proved by novel inequality methods such as, LyapunovCKrasovskii functional and Wirtinger single and double integral inequality. Compared with static trigger conditions, dynamic trigger conditions have more advantages. For example, a new fuzzy filter error system model under dynamic event-triggered control strategy is considered. In addition, there are different triggered thresholds for different fuzzy rules, which can save communication resources more effectively in [26].

In order to realize the synchronization of MNNs, we often add appropriate controllers to the system. According to Tang et al. [27], the leader following consistency problem for a class of nonlinear multiagent systems with mixed impulses and time-varying bounded delays is studied. The time-varying impulses in this paper is not only composed of synchronization impulses and desynchronization impulses but also placed in some nodes of the system. Based on Riemann Liouville derivative, Lyapunov functional method and comparison theorem, we can get the global synchronization problem of time-varying delay neural networks with impulsive fractional complex memristor [10]. The impulse controller is one of the most widely used controllers in recent years. Different from the traditional continuous control strategy, impulse control mechanism has the advantage of short action time, which makes it possible to use the impulse controller to occupy less communication resources for a system with a very large amount of information transmission (see [28, 29]). In order to reduce communication bandwidth and save communication costs, a new control strategy based on event-trigger impulse is given. For example, Yi et al. [30] proposed an impulsive control mechanism based on ETC. Except for above control strategy, the impulse coupling protocol is also studied. The coupling between neural networks only occurs at some discrete-time instants, that is, impulse instants. Consequently, the impulse coupling scheme is naturally proposed.

Observer-based output feedback control is one of the traditional hot topics. It can be divided into two categories according to whether the variables are measurable or not. For the former, a relaxed stability condition based on state observer is proposed [31], and for the latter, a scheme based on fuzzy controller for a class of nonlinear systems is presented [32]. More recently, it is usually presumed that MAS state is measurable. Due to the limitations of measurement methods, many states cannot be measured. On the other hand, system states are unavailable for the state feedback control or too expensive to measure. Thus, it is imperative to research the observer for the system state is not measurable.

In general, we design an observer to estimate the value of different MNNs and then use the information to establish an observer based on feedback controller. However, the measured value is usually collected in discrete time. Therefore, an impulse observer is promoted. It was first proposed by Raf and Allgower in [33]. The observer is updated in the form of impulsive; hence, the measured output is discrete. So, use the impulse observer to estimate the error. Apart from this, designing a suitable control scheme based on impulsive observer is still a challenging problem.

Motivated by the previous research, this paper studies synchronization problem of MNNs with observer via an ETC mechanism. The main contributions of this paper are as follows:

(1) An impulsive switching controller is designed via the event-triggered strategy of MNNs with disconnection switching topology. Considering the practical needs, the actual state may be unpredictable in reality. Thus, the system state in this paper is assumed to be unmeasurable.

(2) A particular observer is constructed. Considering the unknown time delay in practical application, the observer does not exhibit time delay. Through the observation value of synchronization error and the tracking error of synchronization error, an augmented system is formed. The synchronization (quasi-synchronization) of the augmented system is also of the MNN system.

(3) The MNNs with a switching topology is studied and the topology is disconnect. At the same time, impulse control, event-triggered strategies, and observers are used to study synchronization (quasisynchronization) issues. In the real system, the sufficient conditions of the synchronization (quasi-synchronization) are proved. We discuss this kind of question and give the relevant theorems. The Zeno behavior can be ruled out.

The remainder of this article is organized as follows. Section 2 describes problem formulation and some necessary preliminaries. In Section 3, a number of results are presented. In Section 4, a numerical simulation is presented to test the obtained theoretical analysis. Some conclusions are drawn in Section 5.

2. Preparation and Modeling

Notations. Throughout this study, sign( ) is the standard sign function. $\mathbb{Z}$ and $\mathbb{Z}_+$ represent a set of integer and positive integer. $\mathbb{R}^n$ represents n-dimensional Euclid space. $\|\cdot\|$

represents 1-norm. $\mathrm{sign}(x) = (\mathrm{sign}(x_1), \mathrm{sign}(x_2), \ldots, \mathrm{sign}(x_n))^T$, and thus $\|x\| = \mathrm{sign}(x)^T x$ where $x \in \mathbb{R}^n$, and I is an identity matrix. Let $\mathscr{G} = (\mathscr{F}, \mathscr{S})$ denote a graph. $\mathscr{F}$ is the set of nodes. $\mathscr{S} \subseteq \mathscr{F} \times \mathscr{F}$ is the set of edges. An arbitrary matrix $A = (a_{ij})_{N\times N} \in R^{N\times N}$ is given, corresponding to A, and thus from $\mathscr{G}(A) = (\mathscr{F}, \mathscr{S})$, the graph is indicated, where $(i, j) \in \mathscr{S}$ if and only if $a_{ij} > 0$.

Also, a subset $\mathscr{K} \subseteq \mathscr{F}$ and a graph $\mathscr{G} = (\mathscr{F}, \mathscr{S})$ are given. Define the neighborhood of $\partial(\mathscr{K}, \mathscr{G})\{k \in \mathscr{F}/\mathscr{K} | \exists i \in \mathscr{K}$, such that $(i, k) \in \mathscr{S}\}$. If $\mathscr{K}$ is a singleton set, $\partial(\mathscr{K}, \mathscr{G})$ represents the neighborhood of one single point.

When $(j, i) = (i, j)$, the graph $\mathscr{G}$ is undirected. $\mathscr{G} = (\mathscr{F}, \mathscr{S})$ has a directed path from node i to j if there is a sequence of edges in the form (i, i_1), (i, i_2), $\cdots$, (i, i_k) and the $i_p \in N$, where$p = 1, 2, \ldots, k$, $\mathscr{G}$ is called connected if there exists a directed path between each pair of nodes. The node $\hat{r}$ is called a root of $\mathscr{G}$ if has a directed path from $\hat{r}$ to every other node $\mathscr{G}$ contains a directed spanning tree if there exists at least one root.

For the graphs $\mathscr{G}_1 = (\mathscr{F}, \mathscr{S}_1)$ and $\mathscr{G}_2 = (\mathscr{F}, \mathscr{S}_2)$, $\mathscr{G}_1 \cup \mathscr{G}_2 = (\mathscr{F}, \mathscr{S}_1 \cup \mathscr{S}_2)$ is the union of $\mathscr{G}_1$, $\mathscr{G}_2$. A sequence of graphs with common nodes $(\mathscr{G}_i)_{i=1}^m$ is jointly connected if $\cup_{i=1}^m \mathscr{G}_i$ contains a spanning tree. A sequence of graphs with common nodes $(\mathscr{G}_i)_{i=1}^m$ is sequentially connected if there exist $m+1$node sets $\mathscr{F}_0, \mathscr{F}_1, \ldots, \mathscr{F}_m$such that $\mathscr{F}_{k+1} \subseteq \partial(\mathscr{G}_{k+1}, \Omega_k)$ and $\Omega_k = \cup_{l=0}^k \mathscr{F}_l$, $\Omega_0 = \mathscr{F}_0$is a set of Singleton, $\Omega_m = \mathscr{F}$.

Then, by the following dynamics:

$$\frac{\mathrm{d}x_i}{\mathrm{d}t} = Ax_i(t) + Bx_i(t - \tau(t)) + u_i(t) + I(t), \tag{1}$$

where $t \geqslant t_0$, $i \in \mathscr{F} = \{1, 2, \ldots, N\}$, $x_i(t) = (x_{i1}(t), x_{i2}(t), \ldots, x_{in}(t))^T$, $A = (a_{ij})_{n\times n}$ and $B = (b_{ij})_{n\times n}$ are weight matrices; $\tau(t)$ is transmission delay and satisfies $\tau \geqslant \tau(t) \geqslant 0$; $u_i(t)$ is a controller; and $I(t) \in \mathbb{R}^n$ indicates external input.

In the actual situation, considering that the system state value cannot be measured, we give the observer of the corresponding ith node as follows:

$$\frac{\mathrm{d}\hat{x}_i(t)}{\mathrm{d}t} = A\hat{x}_i(t) + v_i(t) + I(t). \tag{2}$$

$\hat{x}_i(t) = (\hat{x}_{i1}(t), \hat{x}_{i2}(t), \ldots, \hat{x}_{in}(t))^T$ is the estimated value of the corresponding ith node. $v_i(t) \in \mathbb{R}^n$ is the controller of the observer. Under (2), we can see that the observer does not contain time-delay term. Considering the fact that the time delay is unknown in practical application, observer (2) does not contain time delay.

Let $S \subset \mathbb{Z}_+$ be a limited set of index and $\{\mathscr{G}_s\colon s \in S\}$ be a directed graph set. $\sigma(t)\colon [t_0, +\infty) \longrightarrow S$ represent function of switching in $\{\mathscr{G}_s\colon s \in S\}$, and $\{t_p = qh, q \in \mathbb{Z}_+\}$ (where $h > 0$) represent instants of switching impulsive time. Let $\mathscr{G}_{\sigma(t)}$ indicate the graph of directed at t, where $t \geqslant t_0$. Thus, obviously $t = t_q$ is the switch time unchanged for $t \in (t_q, t_{q+1})$. We use $(\varpi_{ij}^{\sigma(t)})_{N\times N}$ to express $\mathscr{G}_{\sigma(t)}$ of adjacent matrix, where $\varpi_{ij}^{\sigma(t)} = 1$ when the system sends information from node j to node i and $\varpi_{ij}^{\sigma(t)} = 0$ otherwise. In addition, we give $\varpi_{ii}^{\sigma(t)} = 0$, namely, there is no self-loop in $\mathscr{G}_{\sigma(t)}$ where $t \geqslant t_0$. In order to convenient calculation, we assume that $\varpi_i^{\sigma(t)} = \sum_{j=1}^N \varpi_{ij}^{\sigma(t)}$ and $\varpi = \sup_{t\geqslant t_0} \max_{i\in\mathscr{F}} \varpi_i^{\sigma(t)}$

Consider the following assumptions:

(A1) The set of discrete graphs $\{\mathscr{G}_{\sigma(t)}\colon t_{mT} \leqslant t < t_{(m+1)T}\}$ is sequentially connected, if there exists a positive integer $T \in \mathbb{Z}_+$, where $m \in \mathbb{Z}_+$.

(A2) The set of discrete graphs $\{\mathscr{G}_{\sigma(t)}\colon t_{mT_0} \leqslant t < t_{(m+1)T_0}\}$ is jointly connected, if there exists a positive integer $T_0 \in \mathbb{Z}_+$, where $m \in \mathbb{Z}_+$.

$\{t_q^i\}_{q=1}^{+\infty}$ denotes a sequence of triggering time. Hence, we will give the event-trigger protocol (ETP). In order to make the system achieve synchronization (quasi-synchronization), we design the impulsive switching controller with ETP and the controller of the corresponding observer. In order to make the system achieve synchronization (quasi-synchronization), we design the impulsive switching controller and the corresponding observer controller of the ith node as follows:

$$u_i(t) = \gamma \sum_{q=1}^{+\infty} \delta(t - t_k) \sum_{j=1}^{N} \varpi_{ij}^{\sigma(t)} \left(\hat{x}_j(t_q^i) - \hat{x}_i(t_q^i)\right), \tag{3}$$

$$v_i(t) = \eta \sum_{q=1}^{+\infty} \delta(t - t_k) \sum_{j=1}^{N} \varpi_{ij}^{\sigma(t)} \left(\hat{x}_j(t_q^i) - \hat{x}_i(t_q^i)\right), \tag{4}$$

where $\gamma > 0, \eta > 0$.

The state is not measurable.

Therefore, (3) and (4) are only related to the observed values. For$i \in \mathscr{V}$, the measurement error is defined as follows:

$$\Lambda_i(t) = \sum_{j=1}^{N} \varpi_{ij}^{\sigma(t)} \left(\hat{x}_j(t_q^i) - \hat{x}_i(t_q^i)\right) - \sum_{j=1}^{N} \varpi_{ij}^{\sigma(t)} \left(\hat{x}_j(t) - \hat{x}_i(t)\right). \tag{5}$$

Meanwhile, by Figure 1, we can get the block diagram for ETC and the ETP:

$$t_{q+1}^i = \inf\left\{t > t_q^i, \|\Lambda_i(t)\| > \beta e^{-\varsigma(t-t_0)} + \alpha\right\}, \tag{6}$$

where $\varsigma > 0$, $\alpha^2 + \beta^2 \neq 0$; moreover, $\alpha \geqslant 0$ and $\beta \geqslant 0$. They are both threshold parameters.

From (1)–(4), we have

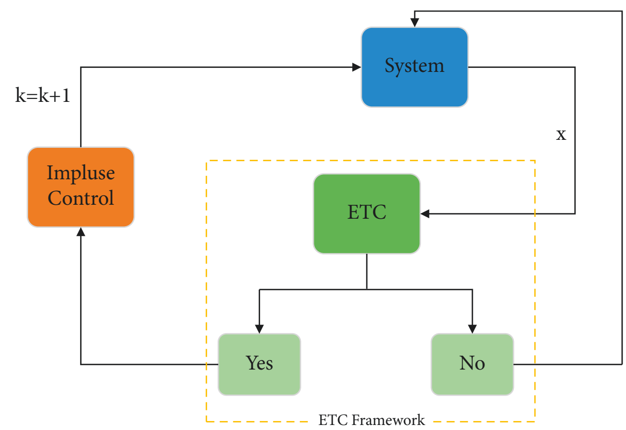

FIGURE 1: The block diagram for ETC.

$$\begin{cases} \dfrac{dx_i}{dt} = Ax_i(t) + Be_{ij}(t-\tau(t)) + I, & t \neq t_k, \\ \widehat{x}_i(t_k^+) = x_i(t_k) + \gamma \sum_{j=1}^{N} \varpi_{ij}^{\sigma(t)} \left(\widehat{x}_j(t_q^i) - \widehat{x}_i(t_q^i)\right), & t = t_k, \end{cases} \tag{7}$$

$$\begin{cases} \dfrac{d\widehat{x}_i(t)}{dt} = A\widehat{x}_i(t) + I, & t \neq t_k, \\ x_i(t_k^+) = x_i(t_k) + \eta \sum_{j=1}^{N} \varpi_{ij}^{\sigma(t)} \left(\widehat{x}_j(t_q^i) - \widehat{x}_i(t_q^i)\right), & t = t_k, \end{cases} \tag{8}$$

where $k \geqslant 1$, $i \in \mathcal{F}$, $t_q^i \leqslant t_k < t_{q+1}^i$, $x_i(t_k^+) = \lim_{t \longrightarrow t_k+0} x_i(t)$, and $x_i(t_k^-) = x_i(t_k)$.

Let C_τ be a Banach space and $C_\tau = C([-\tau, 0], \mathbb{R}^n)$. Let φ: $[-\tau, 0] \longrightarrow \mathbb{R}^n$ represent all continuity functions, and thus the initial value of (7) and (8) can be given:

$$\begin{aligned} x_i(t_0 + \theta) &= \varphi_i(\theta), \quad \theta \in [-\tau, 0], \\ \widehat{x}_i(t_0) &= \widehat{\varphi}_i(t_0), \quad i = 1, \ldots, N, \end{aligned} \tag{9}$$

for $\varphi_i \in C_\tau$ and $\widehat{\varphi}_i(t_0) \in \mathbb{R}^n$. Let $e_{ij}(t) = x_i(t) - x_j(t)$ denote the synchronization error for $i, j \in \mathcal{F}$, where $t \geqslant t_0$ and $\widehat{e}_{ij}(t) = \widehat{x}_i(t) - \widehat{x}_j(t)$ denotes the observed value of $e_{ij}(t)$.

Then,

$$\begin{cases} \dfrac{de_{ij}(t)}{dt} = Ae_{ij}(t) + Be_{ij}(t-\tau(t)), \quad t \neq t_k, \\ e_{ij}(t_k^+) = e_{ij}(t_k) + \gamma \left(\sum_{v=1}^{N} \varpi_{iv}^{\sigma(t)} \left(\widehat{x}_v(t_q^i) - \widehat{x}_i(t_q^i)\right) - \sum_{v=1}^{N} \varpi_{jv}^{\sigma(t)} \left(\widehat{x}_v(t_q^j) - \widehat{x}_j(t_q^j)\right) \right) \\ = e_{ij}(t_k) + \gamma \left(\sum_{v=1}^{N} \varpi_{iv}^{\sigma(t)} \left(\widehat{e}_{vj}(t_k) - \widehat{e}_{ij}(t_k)\right) + \sum_{v=1}^{N} \varpi_{jv}^{\sigma(t)} \left(\widehat{e}_{iv}(t_k) - \widehat{e}_{ij}(t_k)\right) \right) + \gamma\left(\Lambda_i(t_k) - \Lambda_j(t_k)\right), \quad t = t_k, \end{cases} \tag{10}$$

$$\begin{cases} \dfrac{d\widehat{e}_{ij}(t)}{dt} = A\widehat{e}_{ij}(t), \quad t \neq t_k, \\ \widehat{e}_{ij}(t_k^+) = \widehat{e}_{ij}(t_k) + \eta \left(\sum_{v=1}^{N} \varpi_{iv}^{\sigma(t)} \left(\widehat{x}_v(t_q^i) - \widehat{x}_i(t_q^i)\right) - \sum_{v=1}^{N} \varpi_{jv}^{\sigma(t)} \left(\widehat{x}_v(t_q^j) - \widehat{x}_j(t_q^j)\right) \right) \\ = \widehat{e}_{ij}(t_k) + \eta \left(\sum_{v=1}^{N} \varpi_{iv}^{\sigma(t)} \left(\widehat{e}_{vj}(t_k) - \widehat{e}_{ij}(t_k)\right) + \sum_{v=1}^{N} \varpi_{jv}^{\sigma(t)} \left(\widehat{e}_{iv}(t_k) - \widehat{e}_{ij}(t_k)\right) \right) + \eta\left(\Lambda_i(t_k) - \Lambda_j(t_k)\right), \quad t = t_k. \end{cases} \tag{11}$$

Let $\xi_{ij}(t) = e_{ij}(t) - \hat{e}_{ij}(t)$ denote tracking error of synchronization error of ith node and jth node.

Then,

%

$$
\begin{cases}
\dfrac{d\xi_{ij}(t)}{dt} = A\xi_{ij}(t) + Be_{ij}(t-\tau(t)), & t \neq t_k, \\
\xi_{ij}(t_k^+) = \xi_{ij}(t_k) + (\gamma-\eta)\left(\sum_{v=1}^{N} \varpi_{iv}^{\sigma(t)}\left(\hat{e}_{vj}(t_k) - \hat{e}_{ij}(t_k)\right) + \sum_{v=1}^{N} \varpi_{jv}^{\sigma(t)}\left(\hat{e}_{iv}(t_k) - \hat{e}_{ij}(t_k)\right)\right) + (\gamma-\eta)\left(\Lambda_i(t_k) - \Lambda_j(t_k)\right), & t = t_k.
\end{cases}
\tag{12}
$$

Let $W_{ij}(t) = \begin{pmatrix} \hat{e}_{ij}(t) \\ \xi_{ij}(t) \end{pmatrix}$; from (10) and (11), there are the following augmentation systems:

$$
\begin{cases}
\dfrac{dW_{ij}(t)}{dt} = \begin{bmatrix} A & 0 \\ 0 & A \end{bmatrix}\begin{pmatrix} \hat{e}_{ij}(t) \\ \xi_{ij}(t) \end{pmatrix} + \begin{bmatrix} 0 & 0 \\ B & B \end{bmatrix}\begin{pmatrix} \hat{e}_{ij}(t-\tau(t)) \\ \xi_{ij}(t-\tau(t)) \end{pmatrix}, & t \neq t_k, \\
W_{ij}(t_k^+) = \begin{bmatrix} I & 0 \\ 0 & I \end{bmatrix}\begin{pmatrix} \hat{e}_{ij}(t_k) \\ \xi_{ij}(t_k) \end{pmatrix} + \begin{bmatrix} I\eta & 0 \\ I(\gamma-\eta) & 0 \end{bmatrix}\sum_{v=1}^{N} \varpi_{iv}^{\sigma(t)}\left(\begin{pmatrix} \hat{e}_{vj}(t_k) \\ \xi_{vj}(t_k) \end{pmatrix} - \begin{pmatrix} \hat{e}_{ij}(t_k) \\ \xi_{ij}(t_k) \end{pmatrix}\right) & \\
+ \begin{bmatrix} I\eta & 0 \\ I(\gamma-\eta) & 0 \end{bmatrix}\sum_{v=1}^{N} \varpi_{jv}^{\sigma(t)}\left(\begin{pmatrix} \hat{e}_{iv}(t_k) \\ \xi_{iv}(t_k) \end{pmatrix} - \begin{pmatrix} \hat{e}_{ij}(t_k) \\ \xi_{ij}(t_k) \end{pmatrix}\right) + \begin{bmatrix} I\eta & 0 \\ I(\gamma-\eta) & 0 \end{bmatrix}\begin{pmatrix} \Lambda_i(t_k) - \Lambda_j(t_k) \\ \Lambda_i(t_k) - \Lambda_j(t_k) \end{pmatrix}, & t = t_k.
\end{cases}
\tag{13}
$$

In addition, assume that $C_1 = \begin{bmatrix} A & 0 \\ 0 & A \end{bmatrix}$, $C_2 = \begin{bmatrix} 0 & 0 \\ B & B \end{bmatrix}$, $C_3 = \begin{bmatrix} I\eta & 0 \\ I(\gamma-\eta) & 0 \end{bmatrix}$ and $\nabla_i(t) = \begin{pmatrix} \Lambda_i(t) \\ \Lambda_i(t) \end{pmatrix}$ where $i \in \mathscr{F}$ and $t \geqslant t_0$.

Thus, from (13), it follows that

$$
\begin{cases}
\dfrac{dW_{ij}(t)}{dt} = C_1 W_{ij}(t) + C_2 W_{ij}(t-\tau(t)), & t \neq t_k, \\
W_{ij}(t_k^+) = W_{ij}(t_k) + C_3\left(\sum_{v=1}^{N} \varpi_{iv}^{\sigma(t)}\left(W_{vj}(t_k) - W_{ij}(t_k)\right) + \sum_{v=1}^{N} \varpi_{jv}^{\sigma(t)}\left(W_{iv}(t_k) - W_{ij}(t_k)\right)\right) + C_3\left(\nabla_i(t_k) - \nabla_j(t_k)\right), & t = t_k.
\end{cases}
\tag{14}
$$

Definition 1. (14) is called to achieve final synchronization, if $\lim_{t\longrightarrow\infty}\|W_{ij}(t)\| = 0$.

Definition 2. (14) is called to achieve final quasi-synchronization, if $\lim_{t\longrightarrow\infty}\|W_{ij}(t)\| \leqslant a$, where $a > 0$.

Remark 1. From augmented matrix (14), we can find that there are $\lim_{t\longrightarrow\infty}\|e_{ij}(t)\| = 0\,(\lim_{t\longrightarrow\infty}\left\|e_{ij}(t)\right\| \leqslant a)$ if $\lim_{t\longrightarrow\infty}\|W_{ij}(t)\| = 0\,(\lim_{t\longrightarrow\infty}\left\|W_{ij}(t)\right\| \leqslant a)$ for any $i, j \in \mathscr{F}$. The synchronization (quasi-synchronization) of augmented system (13) is also of (1). Moreover, $\lim_{t\longrightarrow\infty}\|e_{ij}(t)\| = 0$ by observer of error systems $\hat{e}_{ij}(t)$ and $\xi_{ij}(t)$ of tracking error of error system. We do not directly quote the state of the error system, and thus it has certain significance for the system. Its state is not measurable in practical application. For notational convenience, we denote $\varpi_{ij}^{\sigma(t_k)} = d_{ij}(t_k)$ at any time instant t_k for $i, j \in \mathcal{F}$, and $\mathcal{G}_k$ denotes $\mathcal{G}_{\sigma(t_k)}$.

3. Main Results

where $\widetilde{W}(t) = \sup_{-\tau\leqslant\theta\leqslant 0} W(t+\theta)$.where $0 < \zeta \leqslant \min\{2\|C_3\|, 1 - 4\|C_3\|\varpi\}$.

Lemma 1. *A sequence of graphs $\{\mathcal{G}_j\}_{j=1}^{T_0}$ is jointly connected if a sequence of graphs $\{\mathcal{G}_j\}_{j=1}^{T}$ is sequentially connected.*

Lemma 2. *There exists $l > 0$ such that*

$$l + \|C_2\| e^{l\tau} + d_1 \leqslant 0, \tag{15}$$

for any $i, j \in \mathcal{F}$ and $t \in (t_k, t_{k+1}]$ where d_1 denotes the largest eigenvalue of C_1, and we obtain that

$$\left\|W_{ij}(t)\right\| \leqslant \left\|\widetilde{W}_{ij}(t)\right\| \leqslant \left\|\widetilde{W}_{ij}(t_k^+)\right\| e^{-l(t-t_k)}. \tag{16}$$

Proof. Let $V(t) = \|W_{ij}(t)\| e^{l(t-t_k)}$ for $t \in (t_k, t_{k+1})$. From (14), we can deduce

$$\begin{aligned}\frac{\mathrm{d}V(t)}{\mathrm{d}t} &= \mathrm{sign}\big(W_{ij}(t)\big)^T \frac{dW_{ij}(t)}{dt} e^{l(t-t_k)} + lV(t)\\ &= \mathrm{sign}\big(W_{ij}(t)\big)^T C_1 W_{ij}(t) e^{l(t-t_k)} + \mathrm{sign}\big(W_{ij}(t)\big)^T C_2 W_{ij}(t-\tau(t)) e^{l(t-t_k)} + lV(t)\\ &\leqslant d_1 V(t) + \|C_2\| V(t-\tau(t)) e^{l\tau} + lV(t).\end{aligned} \tag{17}$$

Here let $\widetilde{V}(t) = \sup_{-\tau\leqslant\theta\leqslant 0} V(t+\theta)$.

We have

$$\frac{\mathrm{d}V(t)}{\mathrm{d}t} \leqslant \left(d_1 + \|C_2\| e^{l\tau} + l\right)\widetilde{V}(t) \leqslant 0. \tag{18}$$

Then, one has $\mathrm{d}\widetilde{V}(t)/\mathrm{d}t \leqslant 0$, and so $\|W_{ij}(t)\| e^{l(t-t_k)} = V(t) \leqslant V(t_k^+) \leqslant \widetilde{V}(t_k^+) = \|\widetilde{W}_{ij}(t_k^+)\|$, i.e., $\|W_{ij}(t)\| \leqslant \|\widetilde{W}_{ij}(t_k^+)\| e^{-l(t-t_k)}$. The proof is completed.

From Assumption (A2), there exists a sequence of graphs $\{\mathcal{G}_j\}_{j=mT+1}^{(m+1)T}$ which is sequentially connected where $m \in \mathbb{Z}_+$. Hereafter, $\mathcal{G}_r^m$ represents $\mathcal{G}_{mT+r}$. A sequence of graphs $\{\mathcal{G}_r^m\}_{r=1}^T$ is sequentially connected for any $m \in \mathbb{Z}_+$; meanwhile, $\Omega_T^m = \mathcal{F}$ and Ω_0^m is a set of singleton.

Let

$$\begin{aligned}\mathcal{H}(t) &= \max_{i,j\in\mathcal{F}} \left\|W_{ij}(t)\right\|,\\ \widetilde{\mathcal{H}}(t) &= \sup_{\theta\in[-\tau,0]} \mathcal{H}(t+\theta),\\ \mathcal{H}_r^m &= \mathcal{H}(t_{mT+r}),\\ \mathcal{H}_r^{m+} &= \mathcal{H}(t_{mT+r}^+),\\ \mathcal{H}_r^m(t) &= \max_{i,j\in\Omega_r^m} \left\|W_{ij}(t)\right\|,\\ \widetilde{\mathcal{H}}_r^m(t) &= \sup_{\theta\in[-\tau,0]} \mathcal{H}_r^m(t+\theta),\\ \mathcal{H}_r^m &= \mathcal{H}(t_{mT+r}),\\ \mathcal{H}_r^{m+} &= \mathcal{H}_{r+1}(t_{mT+r}^+),\end{aligned} \tag{19}$$

where $0 \leqslant r \leqslant T-1$ and $m \in \mathbb{Z}_+$. □

Lemma 3. *By Assumption (A2), if$0 < \|C_3\| < 1/2\varpi$, then*

$$\left\|W_{ij}(t_k^+)\right\| \leqslant \zeta \mathcal{H}_r^m(t_k) + (1-\zeta)\mathcal{H}(t_k) + 4\left\|C_3\right\|\left(\beta e^{-\varsigma(mT+r)h} + \alpha\right), \tag{20}$$

wherem $\in \mathbb{Z}_+, 0 \leqslant r \leqslant T-1, t_q^i \leqslant t_{mT+r} < t_{q+1}^i, q \in \mathbb{Z}_+$, and$0 < \zeta \leqslant \min\{\|C_3\|, 1 - 2\varpi\|C_3\|\}$.

Proof. First, we review the state equation of (14) at the impulse instant.

$$W_{ij}(t_k^+) = W_{ij}(t_k) + C_3\left(\sum_{v=1}^N \varpi_{iv}^{\sigma(t)}\big(W_{vj}(t_k) - W_{ij}(t_k)\big) + \sum_{v=1}^N \varpi_{jv}^{\sigma(t)}\big(W_{iv}(t_k) - W_{ij}(t_k)\big)\right) + C_3\big(\nabla_i(t_k) - \nabla_j(t_k)\big), \tag{21}$$

for $t_q^i \leqslant t_k < t_{q+1}^i$ and $q \in \mathbb{Z}_+$.

Considering $i, j \in \Omega_{r+1}^m$ and $t_k = mT + r$, where $\Omega_{r+1}^m = \Omega_r^m \cup \mathcal{F}_{r+1}^m$, we give the following three cases. □

Case 1. For $i, j \in \Omega_r^m$, under (21), we get

$$\left\|W_{ij}(t_k^+)\right\| \leqslant \operatorname{sign}\left(W_{ij}(t_k^+)\right)^T W_{ij}(t_k) + 2\|C_3\|\varpi\left(\mathscr{H}(t_k) - \operatorname{sign}W_{ij}(t_k^+)^T W_{ij}(t_k)\right) + \|C_3\|\left[\left\|\nabla_i(t_k)\right\| + \left\|\nabla_j(t_k)\right\|\right]. \tag{22}$$

From (6), ETP, and ∇_i, we deduce

$$\left\|\nabla_i\right\| \leqslant 2\left(\beta e^{-\varsigma(t-t_0)} + \alpha\right), \tag{23}$$

for $t \in [t_q^i, t_{q+1}^i)$. Hence, due to (22), we have

$$\begin{aligned}\left\|W_{ij}(t_k^+)\right\| \leqslant{}& \left(1 - 2\|C_3\|\varpi\right)\left\|W_{ij}(t_k)\right\| + 2\|C_3\|\varpi\mathscr{H}(t_k) \\ &+ 4\left\|C_3\right\|\left(\beta e^{-\varsigma(t_k-t_0)} + \alpha\right).\end{aligned} \tag{24}$$

From $0 < \zeta \leqslant \min\{\|C_3\|, 1 - 2\varpi\|C_3\|\}$ and $\mathscr{H}_r^m(t_k) \leqslant \mathscr{H}(t_k)$, we can deduce

$$\begin{aligned}\left\|W_{ij}(t_k^+)\right\| \leqslant{}& \zeta\mathscr{H}_r^m(t_k) + (1-\zeta)\mathscr{H}(t_k) \\ &+ 4\left\|C_3\right\|\left(\beta e^{-\varsigma(t_k-t_0)} + \alpha\right).\end{aligned} \tag{25}$$

Therefore, (20) is established.

Case 2. Let $i \in \mathcal{F}_{r+1}^m$, $j \in \Omega_r^m$, and $d_{is}(t_k) = 1$ if a, $s \in \Omega_r^m$.

Under (21), one has

$$\begin{aligned}W_{ij}(t_k^+) ={}& W_{ij}(t_k) + C_3\left(W_{sj}(t_k) - W_{ij}(t_k)\right) + C_3\left(\sum_{v=1,v\neq s}^{N}\varpi_{iv}^{\sigma(t)}\left(W_{vj}(t_k) - W_{ij}(t_k)\right) + \sum_{v=1}^{N}\varpi_{jv}^{\sigma(t)}\left(W_{iv}(t_k) - W_{ij}(t_k)\right)\right) \\ &+ C_3\left(\nabla_i(t_k) - \nabla_j(t_k)\right).\end{aligned} \tag{26}$$

From (26), we can deduce

$$\begin{aligned}\left\|W_{ij}(t_k^+)\right\| ={}& \left(1 - \left\|C_3\right\|\right)\operatorname{sign}\left(W_{ij}(t_k^+)\right)^T W_{ij}(t_k) + \left\|C_3\right\|\mathscr{H}_r^m(t_k) \\ &+ \left\|C_3\right\|(2\varpi - 1)\left(\mathscr{H}(t_k) - \operatorname{sign}\left(W_{ij}(t_k^+)\right)^T W_{ij}(t_k)\right) + \left\|C_3\right\|\left(\left\|\nabla_i(t_k)\right\| + \left\|\nabla_j(t_k)\right\|\right) \\ \leqslant{}& \zeta\mathscr{H}_r^m(t_k) + (1-\zeta)\mathscr{H}(t_k) + 4\left\|C_3\right\|\left(\beta e^{-\varsigma(t_k-t_0)} + \alpha\right).\end{aligned} \tag{27}$$

Hence, (20) is established.

Case 3. $i, j \in \mathcal{F}_{r+1}^m$, $d_{is}(t_k) = 1$, and $d_{jq}(t_k) = 1$ if $s, q \in \Omega_r^m$.

Because

$$W_{sj}(t_k) + W_{iq}(t_k) = W_{sq}(t_k) + W_{ij}(t_k), \tag{28}$$

from (21), we have

$$\begin{aligned}W_{ij}(t_k^+) ={}& W_{ij}(t_k) + C_3\left(W_{sj}(t_k) - W_{ij}(t_k)\right) + C_3\left(W_{iq}(t_k) - W_{ij}(t_k)\right) \\ &+ C_3\left(\sum_{v=1,v\neq s}^{N}\varpi_{iv}^{\sigma(t)}\left(W_{vj}(t_k) - W_{ij}(t_k)\right) + \sum_{v=1,v\neq q}^{N}\varpi_{jv}^{\sigma(t)}\left(W_{iv}(t_k) - W_{ij}(t_k)\right)\right) + C_3\left(\nabla_i(t_k) - \nabla_j(t_k)\right) \\ ={}& W_{ij}(t_k) + C_3\left(W_{sq}(t_k) - W_{ij}(t_k)\right) + C_3\left(\sum_{v=1,v\neq s}^{N}\varpi_{iv}^{\sigma(t)}\left(W_{vj}(t_k) - W_{ij}(t_k)\right) + \sum_{v=1,v\neq q}^{N}\varpi_{jv}^{\sigma(t)}\left(W_{iv}(t_k) - W_{ij}(t_k)\right)\right) \\ &+ C_3\left(\nabla_i(t_k) - \nabla_j(t_k)\right).\end{aligned} \tag{29}$$

By (29),

$$\begin{aligned}\left\|W_{ij}\left(t_k^+\right)\right\| &\leq \left(1-\left\|C_3\right\|\right)\operatorname{sign}\left(W_{ij}\left(t_k^+\right)\right)^T W_{ij}\left(t_k\right)+\left\|C_3\right\|\mathscr{H}_r^m\left(t_k\right)\\ &\quad+\left\|C_3\right\|(2\varpi-2)\left(\mathscr{H}\left(t_k\right)-\operatorname{sign}\left(W_{ij}\left(t_k^+\right)\right)^T W_{ij}\left(t_k\right)\right)+\left\|C_3\right\|\left(\left\|\nabla_i\left(t_k\right)\right\|+\left\|\nabla_j\left(t_k\right)\right\|\right)\\ &\leq \left\|C_3\right\|\mathscr{H}_r^m\left(t_k\right)+\left(1-2\left\|C_3\right\|\varpi+\left\|C_3\right\|\right)\left\|W_{ij}\left(t_k\right)\right\|+\left\|C_3\right\|(2\varpi-2)\mathscr{H}\left(t_k\right)+4\left\|C_3\right\|\left(\beta e^{-\varsigma\left(t_k-t_0\right)}+\alpha\right)\\ &\leq \zeta\mathscr{H}_r^m\left(t_k\right)+(1-\zeta)\mathscr{H}\left(t_k\right)+4\left\|C_3\right\|\left(\beta e^{-\varsigma\left(t_k-t_0\right)}+\alpha\right).\end{aligned} \tag{30}$$

Obviously, (20) holds. Now the proof is completed.

It is always important to assure that Zeno behavior can not be occurred under ETC (3) and (4) in order to prove the synchronization or quasi-synchronization that can be reached by (14).

For error observation (11), it follows that

$$\begin{aligned}\mathscr{G}(t) &= \max_{i,j\in\mathscr{F}}\left\|\widehat{e}_{ij}(t)\right\|,\\ \widetilde{\mathscr{G}}(t) &= \sup_{\theta\in[-\tau,0]}\mathscr{G}(t+\theta),\\ \mathscr{G}_r^m &= \mathscr{G}\left(t_{mT+r}\right),\\ \mathscr{G}_r^{m+} &= \mathscr{G}\left(t_{mT+r}^+\right),\\ \mathscr{Q}_r^m(t) &= \max_{i,j\in\Omega_r^m}\left\|\widehat{e}_{ij}(t)\right\|,\\ \widetilde{\mathscr{Q}}_r^m(t) &= \sup_{\theta\in[-\tau,0]}\mathscr{Q}_r^m(t+\theta),\\ \mathscr{Q}_r^m &= \mathscr{Q}\left(t_{mT+r}\right),\\ \mathscr{Q}_r^{m+} &= \mathscr{Q}\left(t_{mT+r}^+\right).\end{aligned} \tag{31}$$

Theorem 1. *Assume that all the conditions of Lemma 2, hold, and satisfy following conditions:*

C1: $l_2>0$ *and* $l_2+c_1\leqslant 0$

C2: $0<\eta<(1/2\varpi)$

where c_1 *is the maximum eigenvalue of matrix* A, *and thus (14) does not exhibit Zeno behavior. Event-triggered time sequence* $\{t_q^i\}$ *is generated under event-triggered strategy (6), which satisfies* $q\longrightarrow+\infty$ *when* $t_q^i\longrightarrow+\infty$.

Proof. Let $\{t_q^i\}$ be a bounded set and $\{\mathscr{G}(t_q^i)\}$ also be a bounded set. It is assumed that $\mathscr{G}(t_q^i)<D_2$.

For any $i\in\mathscr{F}$, $t\in[t_q^i,t_{q+1}^i)$, there are

$$\begin{aligned}\left\|\Lambda_i(t)\right\| &= \left\|\sum_{v=1}^N\varpi_{iv}^{\sigma(t)}\widehat{e}_{vi}\left(t_q^i\right)-\sum_{v=1}^N\varpi_{iv}^{\sigma(t)}\widehat{e}_{vi}(t)\right\|\\ &= \left\|\sum_{v=1}^N\left(\varpi_{iv}^{\sigma(t)}\widehat{e}_{vi}\left(t_q^i\right)-\varpi_{iv}^{\sigma(t)}\widehat{e}_{vi}(t)\right)\right\|\\ &\leqslant \sum_{v=1}^N\varpi_{iv}^{\sigma(t)}\int_{t_q^i}^t\left\|\dot{\widehat{e}}_{vi}(t)\right\|\mathrm{d}t.\end{aligned} \tag{32}$$

Let $m\in\mathbb{Z}_+$ such that $[t_q^i,t_{q+1}^i)\subset[t_{mT},t_{(m+1)T})$. By (11), $\|\dot{\widehat{e}}_{vi}(s)\|\leqslant D_1\widetilde{\mathscr{G}}(s)$ where $D_1=\|A\|$.

Similar to Lemma 2, there is $l_2+c_1\leqslant 0$, where $l_2>0$ and c_1 is maximum eigenvalue of A. Thus, we can deduce $\widetilde{\mathscr{G}}(s)\leqslant\widetilde{\mathscr{G}}(t_q^{i+})e^{|l_2|(s-t_q^i)}$, where $s\in[t_q^i,t]$ and $\widetilde{\mathscr{G}}(t_q^{i+})=\lim_{s\longrightarrow t_q^i+0}\widetilde{\mathscr{G}}(s)$.

Then, we have

$$\left\|\dot{\widehat{e}}_{vi}(s)\right\|\leqslant D_1\widetilde{\mathscr{G}}\left(t_q^{i+}\right)e^{l_2\left(s-t_q^i\right)}, \tag{33}$$

where $s\in[t_q^i,t]$. Obviously, there are $\widetilde{\mathscr{G}}(t_q^{i+})=\widetilde{\mathscr{G}}(t_q^i)\leqslant D_2$ for $t_q^i\in(t_{mT},t_{(m+1)T})$.

Similar to Lemma 3, at impulse instants, (11) has

$$\mathscr{Q}_r^m\left(t_k^+\right)=\psi\mathscr{Q}_r^m\left(t_k\right)+(1-\psi)\mathscr{G}_r^m\left(t_k\right)+2\eta\left(\beta e^{-\varsigma(mT+r)h}+\alpha\right), \tag{34}$$

if exists $0<\eta<21\varpi$, where $0<\psi\leqslant\min\{\eta,1-2\varpi\eta\}$, if $t_q^i=t_{mT}$, $\widetilde{\mathscr{Q}}_0^m(t_{mT})=\widetilde{\mathscr{G}}_0^m(t_{mT})$ thus

$$\begin{aligned}\widetilde{\mathscr{G}}\left(t_q^{i+}\right) &= \widetilde{\mathscr{G}}_0^{m+}\\ &\leqslant \widetilde{\mathscr{G}}_0^m+2\eta\left[\beta e^{-\varsigma mTh}+\alpha\right]\\ &\leqslant D_2+2\eta\left[\beta e^{-\varsigma mTh}+\alpha\right].\end{aligned} \tag{35}$$

Let $D_2+2\eta[\beta e^{-\varsigma mTh}+\alpha]=\Pi$. Combine (32)–(35), and we have

$$\begin{aligned}\left\|\Lambda_i(t)\right\| &\leqslant D_1\Pi\varpi\int_{t_q^i}^{t} e^{l_2\left(s-t_q^i\right)}\mathrm{d}s \\ &= \frac{D_1\Pi\varpi}{l_2}\left[e^{l_2\left(t-t_q^i\right)}-1\right].\end{aligned} \tag{36}$$

From (6), event-triggered strategy is triggered to update the controller when $\|\Lambda_i(t)\| = \beta e^{-\varsigma(t-t_0)}+\alpha$; in other words, $t_q^i \longrightarrow t_{q+1}^i$. Hence, from (36), we obtain that

$$\begin{aligned}\left\|\Lambda_i\left(t_{q+1}^i\right)\right\| &= \beta e^{-\varsigma\left(t_{q+1}^i-t_0\right)}+\alpha \\ &\leqslant \frac{D_1\Pi\varpi}{l_2}\left[e^{l_2\left(t_{q+1}^i-t_q^i\right)}-1\right],\end{aligned} \tag{37}$$

which means

$$\frac{\left(\beta e^{-\varsigma\left(t_{q+1}^i-t_0\right)}+\alpha\right)l_2}{D_1\Pi\varpi}+1 \leqslant e^{l_2\left(t_{q+1}^i-t_q^i\right)}, \tag{38}$$

and then

$$t_{q+1}^i - t_q^i \geqslant \frac{\ln\left(\left(\left(\beta e^{-\varsigma\left(t_{q+1}^i-t_0\right)}+\alpha\right)l_2/D_1\Pi\varpi\right)+1\right)}{l_2}, \tag{39}$$

such that the event-triggered sequence $\{t_q^i\}$ has time interval. This is contrary to the assumption that the sequence $\{t_q^i\}$ is bounded. This ends the proof. □

Theorem 2. *By Assumption (A1), ifTheorem 1,Lemma 2, andLemma 3hold, then the quasi-synchronization of (7) can be obtained based on observer if* $l \neq 0$*satisfies (15) besides*

$$e^{-lTh}\left(1-\zeta^T\right)<1, \tag{40}$$

where$0<\zeta \leqslant \min\{2\|C_3\|, 1-4\|C_3\|\varpi\}$.

Proof. According to Lemma 2, we can see that

$$\mathscr{H}_{r+1}^m \leqslant \widetilde{\mathscr{H}}_{r+1}^m \leqslant \widetilde{\mathscr{H}}_r^{m+} e^{-lh}, \tag{41}$$

$$\mathscr{H}_{r+1}^m \leqslant \widetilde{\mathscr{H}}_{r+1}^m \leqslant \widetilde{\mathscr{H}}_r^{m+} e^{-lh}, \tag{42}$$

where $m \in \mathbb{Z}_+, 0 \leq r \leq T-1$. By Theorem 1, we can know that Zeno behavior cannot occur.

Meanwhile, according to Lemma 3, it follows that

$$\begin{aligned}\widetilde{\mathscr{H}}_r^{m+} &\leqslant \zeta\widetilde{\mathscr{H}}_r^m + (r-\zeta)\widetilde{\mathscr{H}}_r^m + 4\left\|C_3\right\|\left(\beta e^{-\varsigma(mT+r)h}+\alpha\right), \\ \widetilde{\mathscr{H}}_r^{m+} &\leqslant \widetilde{\mathscr{H}}_r^m + 4\left\|C_3\right\|\left(\beta e^{-\varsigma(mT+r)h}+\alpha\right).\end{aligned} \tag{43}$$

Combining (41) and (43), we can obtain that

$$\widetilde{\mathscr{H}}_{r+1}^m \leqslant e^{-lh}\left[\widetilde{\mathscr{H}}_r^m + 4\left\|C_3\right\|\left(\beta e^{-\varsigma(mT+r)h}+\alpha\right)\right]. \tag{44}$$

Then, from (41)–(44), through the iterative method, we can obtain that

$$\begin{aligned}\widetilde{\mathscr{H}}_r^{m+} &\leqslant e^{-lh}\left[\zeta\widetilde{\mathscr{H}}_{r-1}^{m+} + (1-\zeta)\widetilde{\mathscr{H}}_{r-1}^m\right] + \beta_1 e^{-\varsigma(mT+r-1)h} + \alpha_1 \\ &\leqslant e^{-2lh}\left[\zeta^2\widetilde{\mathscr{H}}_{r-2}^{m+} + \left(1-\zeta^2\right)\widetilde{\mathscr{H}}_{r-2}^m\right] + \beta_2 e^{-\varsigma(mT+r-2)h} + \alpha_2 \\ &\cdots \\ &\leqslant e^{-lvh}\left[\zeta^v\widetilde{\mathscr{H}}_{r-v}^{m+} + (1-\zeta^v)\widetilde{\mathscr{H}}_{r-v}^m\right] + \beta_v e^{-\varsigma(mT+r-v)h} + \alpha_v,\end{aligned} \tag{45}$$

and

$$\begin{aligned}\alpha_1 &= 4\left\|C_3\right\|\alpha\left[(1-\zeta)e^{-lh}+1\right], \\ \alpha_2 &= \left[e^{-2lh}\zeta^2+1\right]\alpha_1 + 4\left\|C_3\right\|(1-\zeta)e^{-2lh}\alpha, \\ &\cdots \\ \alpha_v &= \left[e^{-vlh}\zeta^v+1\right]\alpha_v + 4\left\|C_3\right\|\left(1-\zeta^{v-1}\right)e^{-vlh}\alpha, \\ \beta_1 &= 4\left\|C_3\right\|\left[(1-\zeta)e^{-lh}+e^{-\varsigma h}\right]\beta, \\ \beta_2 &= \left[e^{-2lh}\zeta^2+e^{-2\varsigma h}\right]\beta_1 + 4\left\|C_3\right\|(1-\zeta)e^{-2lh}\beta, \\ &\cdots \\ \beta_v &= \left[e^{-vlh}\zeta^v+e^{-v\varsigma h}\right]\beta_{v-1} + 4\left\|C_3\right\|\left(1-\zeta^{v-1}\right)e^{-vlh}\beta,\end{aligned} \tag{46}$$

and thus

$$\begin{aligned}\widetilde{\mathscr{H}}_T^m &\leqslant e^{-lh}\widetilde{\mathscr{H}}_{T-1}^{m+} \\ &\leqslant e^{-lTh}\left[\zeta^{T-1}\widetilde{\mathscr{H}}_0^{m+} + \left(1-\zeta^{T-1}\right)\widetilde{\mathscr{H}}_0^m\right] + e^{-lh}\beta_{T-1}e^{-\varsigma mTh} \\ &\quad + e^{-lh}\alpha_{T-1}.\end{aligned} \tag{47}$$

From the introduction of the previous preparation part, we have $\Omega_{T-1} = \mathscr{F}$ and $\widetilde{\mathscr{H}}_T^m = \widetilde{\mathscr{H}}_T^m = \widetilde{\mathscr{H}}_0^{m+1}$. Meanwhile, from Ω_0 which is a single point, we can obtain $\widetilde{\mathscr{H}}_0^m = 0$. By using (47), one has

$$\begin{aligned}\widetilde{\mathscr{H}}_0^{m+} &\leqslant \zeta\widetilde{\mathscr{H}}_0^m + (1-\zeta)\widetilde{\mathscr{H}}_0^m + 4\left\|C_3\right\|\left[\beta e^{-\varsigma mTh}+\alpha\right] \\ &\leqslant (1-\zeta)\widetilde{\mathscr{H}}_0^m + 4\left\|C_3\right\|\left[\beta e^{-\varsigma mTh}+\alpha\right].\end{aligned} \tag{48}$$

By applying (47) and (48), we can prove the following result:

$$\widetilde{\mathscr{H}}_0^{m+1} \leqslant \varepsilon\widetilde{\mathscr{H}}_0^m + \overline{\alpha} + \overline{\beta}e^{-m\varsigma Th}, \tag{49}$$

where $0<\varepsilon = e^{-lTh}(1-\zeta^T)<1, \overline{\alpha} = 4\|C_3\|\alpha e^{-lTh} + e^{-lh}\alpha_{T-1}+$, and $\overline{\beta} = e^{-lh}\beta_{T-1} + 4\|C_3\|\beta e^{-lTh}$. From (43), it follows that

$$\begin{aligned}
\widetilde{\mathscr{H}}_0^{m+1} &\leqslant \varepsilon\widetilde{\mathscr{H}}_0^{m} + \overline{\beta}e^{-m\varsigma Th} + \overline{\alpha} \\
&\leqslant \varepsilon^2\widetilde{\mathscr{H}}_0^{m-1} + \overline{\beta}\varepsilon e^{-(m-1)\varsigma Th} + \overline{\beta}e^{-m\varsigma Th} + \varepsilon\overline{\alpha} + \overline{\alpha} \\
&\quad \cdots \\
&\leqslant \varepsilon^{m-1}\widetilde{\mathscr{H}}_0^{2} + \overline{\beta}\varepsilon^{m-2}e^{-2\varsigma Th} + \cdots + \overline{\beta}\varepsilon e^{-(m-1)\varsigma Th} + \overline{\beta}e^{-m\varsigma Th} + \left(\varepsilon^{m-1} + \cdots + \varepsilon + 1\right)\overline{\alpha} \\
&\leqslant \varepsilon^{m}\widetilde{\mathscr{H}}_0^{1} + \frac{e^{-m\varsigma Th} - \varepsilon^m}{1 - \varepsilon e^{\varsigma Th}}\overline{\beta} + \frac{1 - \varepsilon^{m+1}}{1 - \varepsilon}\overline{\alpha}.
\end{aligned} \tag{50}$$

Therefore, we can obtain

$$\lim_{m\longrightarrow\infty} \sup\widetilde{\mathscr{H}}_0^{m} \leqslant \overline{\alpha}. \tag{51}$$

(14) can achieve quasi-synchronization. In other words, (7) can also quasi-synchronization-based observer.

In addition, $\lim_{m\longrightarrow\infty}\sup\widetilde{\mathscr{H}}_0^{m} = 0$ if $\overline{\alpha} = 0$. From Theorem 2, (7) can reach synchronization-based observer if the sufficient conditions are satisfied. □

Remark 2. Under all the conditions of Theorem 2, (14) can be quasi-synchronized. According to the definition of (14), we can find that the system is composed of an observation error system $\widehat{e}_{ij}(t)$ and a tracking error system $\xi_{ij}(t)$. Therefore, when (14) can be quasi-synchronized by means of $\widehat{e}_{ij}(t) and \xi_{ij}(t)$, we can have the quasi-synchronization of (1). In this process, we do not directly use the state value of the original system (1). It is consistent with the situation that the state value of the system is unknown in practical application.

Theorem 3. *Under Assumption (A3), usingLemma 2,Lemma 3, andTheorem 1, system (7) can obtain quasi-synchronization-based observer if*

$$e^{-l(N-1)^2T_0h}\left(1 - \zeta^{(N-1)^2T_0}\right) < 1. \tag{52}$$

Proof. From Lemma 1, when the sequence of graphs $\{\mathscr{G}_j\}_{j=1}^{T_0}$ satisfies $e^{-l(N-1)^2T_0h}(1 - \zeta^{(N-1)^2T_0}) < 1$, the sequence of graphs $\{\mathscr{G}_j\}_{j=1}^{T}$ satisfies $e^{-lTh}(1 - \zeta^T) < 1$. Therefore, under Lemma 2, system (7) can have quasi-synchronization-based observer and can have synchronization if $\alpha = 0$. □

4. Numerical Simulations

In this section, a numerical example is given to verify the validity of theory analyses.

Review original system (7) with controller and observer system (8):

$$\begin{cases}
\dfrac{\mathrm{d}x_i(t)}{\mathrm{d}t} = Ax_i(t) + Bx_i(t - \tau(t)) + I, & t \neq t_k, \\
x_i(t_k^+) = x_i(t_k) + \gamma\displaystyle\sum_{j=1}^{N}\varpi_{ij}^{\sigma(t)}\left(\widehat{x}_j\left(t_q^i\right) - \widehat{x}_i\left(t_q^i\right)\right), & t = t_k,
\end{cases}$$

$$\begin{cases}
\dfrac{\mathrm{d}\widehat{x}_i(t)}{\mathrm{d}t} = A\widehat{x}_i(t) + I, & t \neq t_k, \\
\widehat{x}_i(t_k^+) = \widehat{x}_i(t_k) + \eta\displaystyle\sum_{j=1}^{N}\varpi_{ij}^{\sigma(t)}\left(\widehat{x}_j\left(t_q^i\right) - \widehat{x}_i\left(t_q^i\right)\right), & t = t_k.
\end{cases} \tag{53}$$

Let $i \in \mathscr{F} = \{1, 2, 3, 4, 5, 6, 7, 8\}$, and the parameters in the system are designed as follows: $\gamma = 0.12$ and $\eta = 0.05$, and the weight matrix is designed as

$$A = \begin{pmatrix} -4 & 1 \\ 2 & -3 \end{pmatrix}, \quad B = \begin{pmatrix} 1 & -0.5 \\ -0.5 & 0.8 \end{pmatrix}. \tag{54}$$

Meanwhile, the initial function is given as follows: $\varphi_1 = [0.8, -0.3]^T$, $\varphi_2 = [-0.7, 0.4]^T$, $\varphi_3 = [1.2, -0.5]^T$, $\varphi_4 = [1.3, -0.2]^T$, $\varphi_5 = [0.3, -0.3]^T$, $\varphi_6 = [0.78, -0.5]^T$, $\varphi_7 = [0.42, -0.32]^T$, $\varphi_8 = [-0.4, -0.6]^T$, $\widehat{\varphi}_1 = [1.1, -0.8]^T$, $\widehat{\varphi}_2 = [0.7, -0.78]^T$, $\widehat{\varphi}_3 = [0.45, -1]^T$, $\widehat{\varphi}_4 = [-0.63, 0.9]^T$, $\widehat{\varphi}_5 = [-0.43, -0.56]^T$, $\widehat{\varphi}_6 = [0.7, -1.3]^T$, $\widehat{\varphi}_7 = [0.3, -0.4]^T$, $\widehat{\varphi}_8 = [0.86, -0.3]^T$, and $\tau(t) = |\sin(t)|$, and we set $t_k = 0.5k$, $k\in_+$. Figures 2 and 3 show the switching topology.

From Figure 2 ($\mathscr{G}_{2m}$) and Figure 3 ($\mathscr{G}_{2m+1}$), we can find that $\{\mathscr{G}_{2m}, \mathscr{G}_{2m+1}\}$ is sequential connection. In the switching period $T = 2$, it is also a joint connection and $T_0 = 2$. The change of node set is as follows: $\Omega_0 = \{1\}$, $\Omega_1 = \{1, 4, 5, 8\}$, and $\Omega_2 = \{1, 2, 3, 4, 5, 6, 7, 8\} = \mathscr{V}$. Satisfy Assumptions (A1) and (A2), and the coupling matrix is as follows:

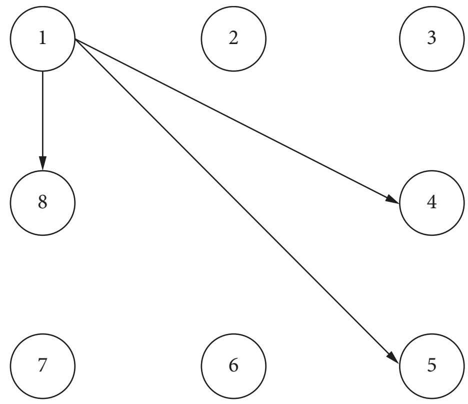

FIGURE 2: $\mathscr{G}_{2m}$.

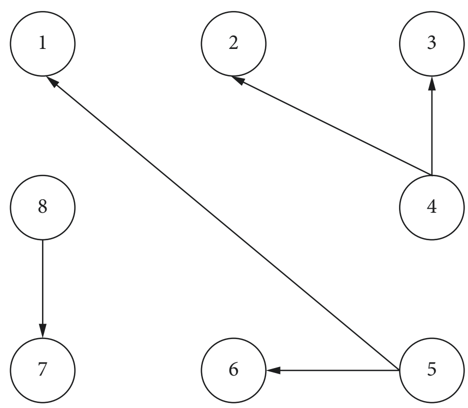

FIGURE 3: $\mathscr{G}_{2m+1}$.

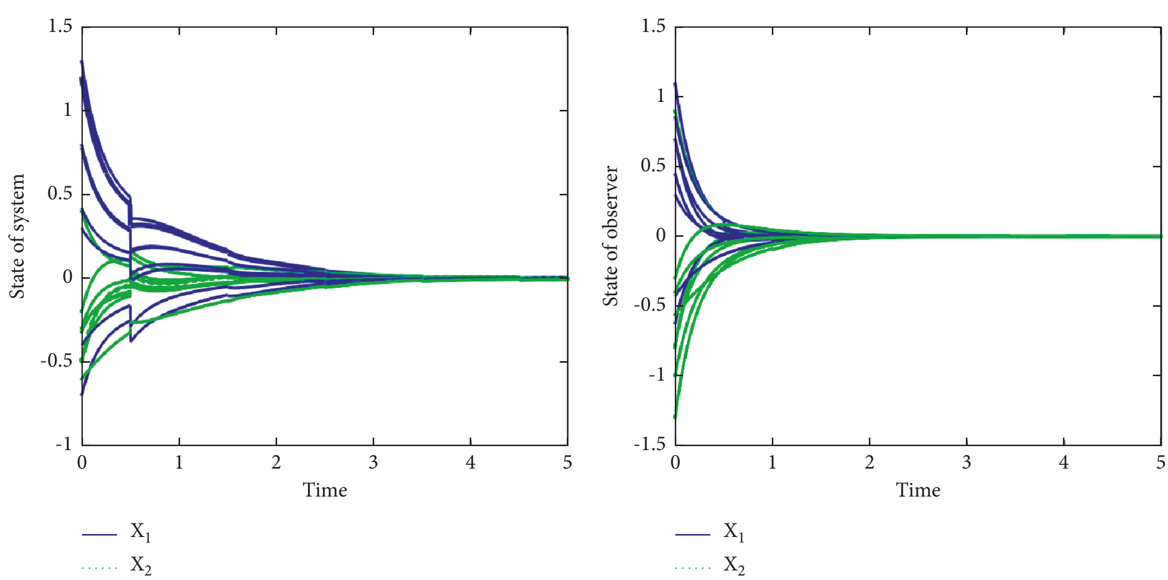

FIGURE 4: The quasi-synchronization. State diagram of 8 nodes of observation system (1) and system (2), when $\alpha = 0.2$.

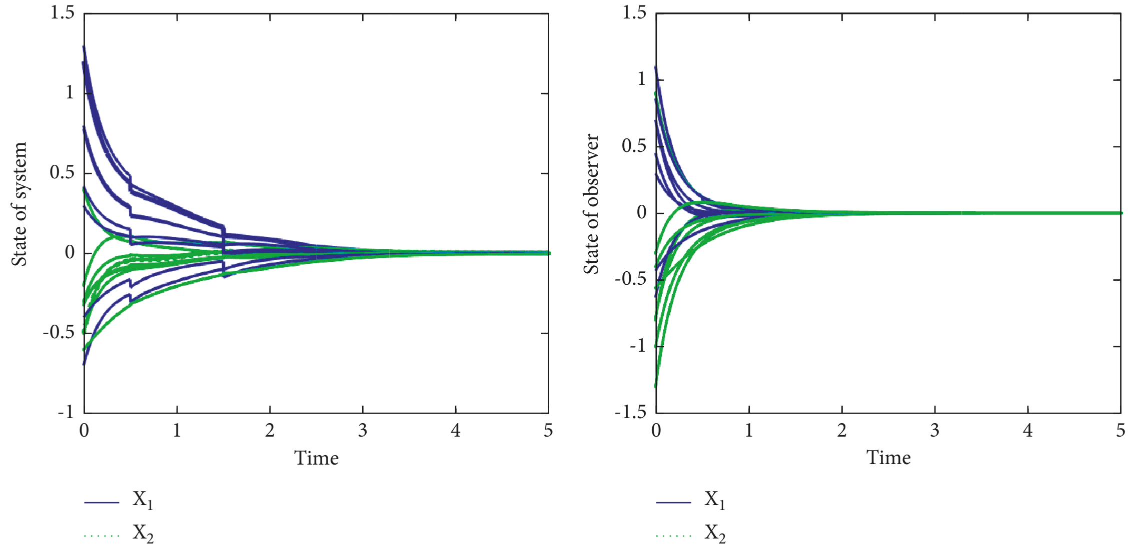

FIGURE 5: The quasi-synchronization. State diagram of 8 nodes of observation system (1) and system (2), when $\alpha = 0$.

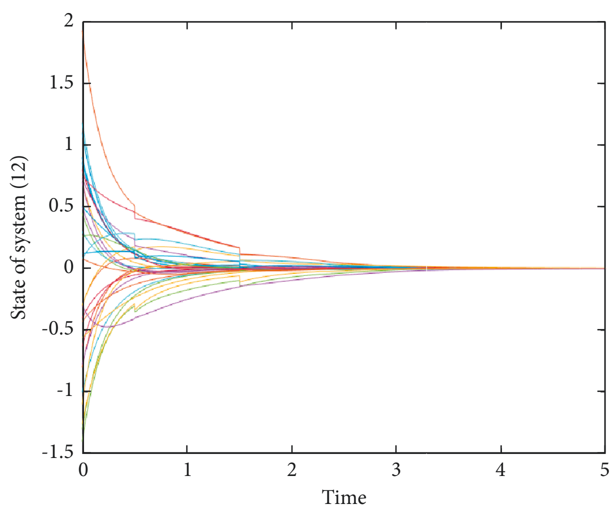

FIGURE 6: The state diagram of 8 nodes of system (14) when $\alpha = 0.2$.

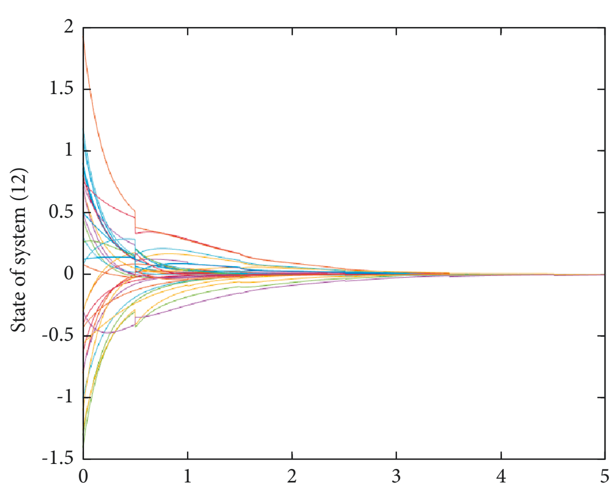

FIGURE 7: The state diagram of 8 nodes of system (14) when $\alpha = 0$.

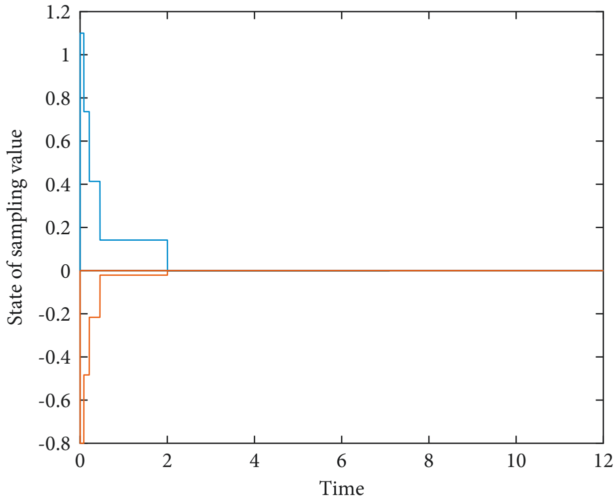

FIGURE 8: The state of sampling value is given when $\alpha = 0.2$.

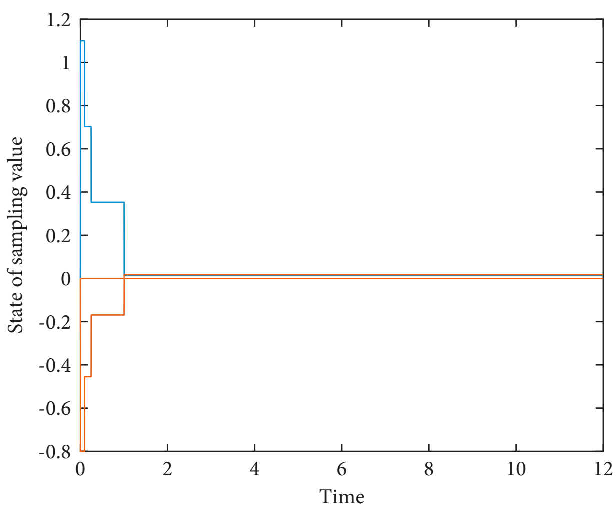

FIGURE 9: The state of sampling value is given when $\alpha = 0$.

$$\mathcal{G}_{2m} = \begin{pmatrix} 0 & 0 & 0 & 1 & 1 & 0 & 0 & 1 \\ 0 & 0 & 0 & 0 & 0 & 0 & 0 & 0 \\ 0 & 0 & 0 & 0 & 0 & 0 & 0 & 0 \\ 0 & 0 & 0 & 0 & 0 & 0 & 0 & 0 \\ 0 & 0 & 0 & 0 & 0 & 0 & 0 & 0 \\ 0 & 0 & 0 & 0 & 0 & 0 & 0 & 0 \\ 0 & 0 & 0 & 0 & 0 & 0 & 0 & 0 \\ 0 & 0 & 0 & 0 & 0 & 0 & 0 & 0 \end{pmatrix},$$

$$\mathcal{G}_{2m+1} = \begin{pmatrix} 0 & 0 & 0 & 0 & 0 & 0 & 0 & 0 \\ 0 & 0 & 0 & 0 & 0 & 0 & 0 & 0 \\ 0 & 0 & 0 & 0 & 0 & 0 & 0 & 0 \\ 0 & 1 & 1 & 0 & 0 & 0 & 0 & 0 \\ 1 & 0 & 0 & 0 & 0 & 1 & 0 & 0 \\ 0 & 0 & 0 & 0 & 0 & 0 & 0 & 0 \\ 0 & 0 & 0 & 0 & 0 & 0 & 0 & 0 \\ 0 & 0 & 0 & 0 & 0 & 0 & 1 & 0 \end{pmatrix}. \tag{55}$$

Thus, we know $\omega = 3$, $T = 2$.

From the above data, augmented matrix (14), we have

$$\begin{aligned} C_1 &= \begin{bmatrix} A & 0 \\ 0 & A \end{bmatrix} = \begin{pmatrix} -4 & 1 & 0 & 0 \\ 2 & -3 & 0 & 0 \\ 0 & 0 & -4 & 1 \\ 0 & 0 & 2 & -3 \end{pmatrix}, \\ C_2 &= \begin{bmatrix} 0 & 0 \\ B & B \end{bmatrix} = \begin{pmatrix} 0 & 0 & 0 & 0 \\ 0 & 0 & 0 & 0 \\ 1 & -0.5 & 1 & -0.5 \\ -0.5 & 0.8 & -0.5 & 0.8 \end{pmatrix}, \\ C_3 &= \begin{bmatrix} I\eta & 0 \\ I(\gamma - \eta) & 0 \end{bmatrix} = \begin{pmatrix} 0.05 & 0 & 0 & 0 \\ 0 & 0.05 & 0 & 0 \\ 0.07 & 0 & 0 & 0 \\ 0 & 0.07 & 0 & 0 \end{pmatrix}. \end{aligned} \tag{56}$$

For Lemma 2, $l + \|C_2\| e^{l\tau} + d_1 = l + 1.5e^{r} - 2 \leq 0$ by solution of the integral equation reach $l < \ = 0.188$. Let $l = 0.15$, and the condition of Lemma 2 can be satisfied.

For Lemma 3, we can obtain $\|C_3\| = 0.12 \leq (1/2\omega) = (1/6)$, and Lemma 3 is also satisfied. According to the conditions in Theorem 1, we have $l_2 + c_1 \leq 0$ and $l_2 \leq 2$. Let $l_2 = 0.15$ and satisfy the condition of Theorem 1. For C2, we have $\eta = 0.05 < (1/2\varpi) = (1/6)$. Thus, according to Theorem 1, there is no Zeno behavior.

For Theorem 2, $0 < \zeta \leq \min\{2\|C_3\|, 1 - 4\|C_3\|\varpi\}$ obtain $\zeta = 0.3$. According to $e^{-lTh}(1 - \zeta^{T}) = e^{-0.15\times 2\times 0.0025}(1 - 0.3^2) < 1$, the condition of Theorem 2 is also established where $h = 0.0025$. Then, (14) can reach the quasi-synchronization, namely, (1) achieves quasi-synchronization based on observers.

Take $\alpha > 0$, $\beta = 2$, and $\varsigma = 0.8$.

Under quasi-synchronization, the state diagram of 8 nodes of (1) and (2) when $\alpha = 0.2$ is shown in Figure 4. Under synchronization, the state diagram of 8 nodes of (1) and (2) when $\alpha = 0$ is shown in Figure 5.

Figure 6 shows the state diagram of 8 nodes of system (14) when $\alpha = 0.2$.

Figure 7 shows the state diagram of 8 nodes of system (14) when $\alpha = 0$.

In Figure 8, the state of sampling value is given when $\alpha = 0.2$. In Figure 9, the state of sampling value is given when $\alpha = 0$. When the system meets the conditions given in this paper, all nodes reach synchronization. Thus, we can find that the theorem given in this article is valid.

5. Conclusion

The question of quasi-synchronization (synchronization) in MNNs with observers in impulsive coupling controller via event-trigger strategy is discussed. An event-triggering mechanism is designed by using the combination measurement method. The real system state in this paper is assumed to be unmeasurable, and the system time delay is also unmeasurable. The state of (1) is measured by observer. The time delay is unknown, so the observer does not have time delay too. The augmented system is composed of the observer and the tracking error system of the error system. In the real system, the sufficient conditions of the quasi-synchronization and synchronization are proved. Compared with existing works, this paper considers the real state and unmeasurable time delay, and the controller used in this paper is a impulsive controller with event-triggered mechanism, so it plays a significant role in saving communication resources. In addition, we consider trying to spread it to the more general system and more complex systems.

Data Availability

No data were used to support this study.

Conflicts of Interest

The authors declare that there are no conflicts of interest regarding the publication of this paper.

Acknowledgments

This study was supported by the Natural Science Foundation of China (62072164 and 11704109).

References

[1] M. Pipattanasomporn, H. Feroze, and S. Rahman, “Multi-agent systems in a distributed smart grid: design and implementation,” in *Proceedings of the 2009 IEEE/PES Power Systems Conference and Exposition*, pp. 1–8, IEEE, Seattle, WA, USA, 15-18 March 2009.

[2] H. Li, A. Mynett, E. Penning, and H. Qi, “Revealing spatial pattern dynamics in aquatic ecosystem modelling with Multi-Agent Systems in Lake Veluwe,” *Ecological Informatics*, vol. 5, no. 2, pp. 97–107, 2010.

[3] W. Ren and N. Sorensen, “Distributed coordination architecture for multi-robot formation control,” *Robotics and Autonomous Systems*, vol. 56, no. 4, pp. 324–333, 2008.

[4] J. A. Fax and R. M. Murray, “Information flow and cooperative control of vehicle formations,” *IEEE Transactions on Automatic Control*, vol. 49, no. 9, pp. 1465–1476, 2004.

[5] M. S. Ali and P. Balasubramaniam, “Exponential stability of uncertain stochastic fuzzy BAM neural networks with time-varying delays,” *Neurocomputing*, vol. 72, no. 4-6, pp. 1347–1354, 2009.

[6] M. S. Ali and R. Saravanakumar, “Improved delay-dependent robust H_∞ control of an uncertain stochastic system with interval time-varying and distributed delays,” *Chinese Physics B*, vol. 23, no. 12, p. 120201, 2014.

[7] K. Hengster-Movric, K. You, F. L. Lewis, and L. Xie, “Synchronization of discrete-time multi-agent systems on graphs using Riccati design,” *Automatica*, vol. 49, no. 2, pp. 414–423, 2013.

[8] Q. Jia, W. K. S. Tang, and W. A. Halang, “Leader following of nonlinear agents with switching connective network and coupling delay,” *IEEE Transactions on Circuits and Systems I: Regular Papers*, vol. 58, no. 10, pp. 2508–2519, 2011.

[9] Z. Meng, W. Ren, Y. Cao, and Z. You, “Leaderless and leader-following consensus with communication and input delays under a directed network topology,” *IEEE Transactions on Systems, Man, and Cybernetics, Part B (Cybernetics)*, vol. 41, no. 1, pp. 75–88, 2011.

[10] M. S. Ali, M. Hymavathi, and S. Senan, “Global asymptotic synchronization of impulsive fractional-order complex-valued memristor-based neural networks with time varying delays,” *Communications in Nonlinear Science and Numerical Simulation*, vol. 78, p. 104869, 2019.

[11] S. Kiranyaz, T. Ince, and O. Abdeljaber, “1-d convolutional neural networks for signal processing applications,” in *Proceedings of the ICASSP 2019-2019 IEEE International Conference on Acoustics, Speech and Signal Processing (ICASSP)*, pp. 8360–8364, IEEE, Brighton, UK, 12-17 May 2019.

[12] F. Cus and U. Zuperl, “Approach to optimization of cutting conditions by using artificial neural networks,” *Journal of Materials Processing Technology*, vol. 173, no. 3, pp. 281–290, 2006.

[13] H. Zhang, Y. Sheng, and Z. Zeng, “Synchronization of coupled reaction-diffusion neural networks with directed topology via an adaptive approach,” *IEEE Transactions on Neural Networks and Learning Systems*, pp. 1–12, 2017.

[14] C. Chen, F. L. Lewis, K. Xie, S. Xie, and Y. Liu, “Off-policy learning for adaptive optimal output synchronization of heterogeneous multi-agent systems,” *Automatica*, vol. 119, p. 109081, 2020.

[15] P. Liu, Z. Zeng, and J. Wang, “Global synchronization of coupled fractional-order recurrent neural networks,” *IEEE Transactions on Neural Networks and Learning Systems*, vol. 30, no. 8, pp. 2358–2368, 2019.

[16] Y. Chen, W. Yu, S. Tan, and H. Zhu, “Synchronizing nonlinear complex networks via switching disconnected topology,” *Automatica*, vol. 70, pp. 189–194, 2016.

[17] J. Chen, B. Chen, and Z. Zeng, “Exponential quasi-synchronization of coupled delayed memristive neural networks via intermittent event-triggered control,” *Neural Networks*, vol. 141, pp. 98–106, 2021.

[18] Y. Xu, J. Liu, and W. Li, “Quasi-synchronization of fractional-order multi-layer networks with mismatched parameters via delay-dependent impulsive feedback control,” *Neural Networks*, vol. 150, pp. 43–57, 2022.

[19] J. Chen, B. Chen, and Z. Zeng, “Event-based synchronization for multiple neural networks with time delay and switching

disconnected topology," *IEEE Transactions on Cybernetics*, vol. 99, pp. 1–11, 2020.
[20] D. A. Hao, B. Jj, and Y. B. Li, "Event-triggered exponential synchronization of complex dynamical networks with cooperatively directed spanning tree topology," *Neurocomputing*, vol. 330, pp. 355–368, 2019.
[21] E. Arslan, R. Vadivel, M. Syed Ali, and S. Arik, "Event-triggeredH∞filtering for delayed neural networks via sampled-data," *Neural Networks*, vol. 91, pp. 11–21, 2017.
[22] R. Vadivel and Y. H. Joo, "Robust event-triggered TCS fuzzy system with successive time-delay signals and its application," *IET Control Theory & Applications*, vol. 14, no. 20, pp. 3697–3712, 2020.
[23] S. Wen, G. Guo, and B. Chen, "Event-triggered cooperative control of vehicle platoons in vehicular ad hoc networks," *Information ences*, pp. 341–353, 2018.
[24] J. Qiang and W. Tang, "Event-triggered protocol for the consensus of multi-agent systems with state-dependent nonlinear coupling[J]," *IEEE Transactions on Circuits and Systems I: Regular Papers*, vol. 65, no. 99, pp. 723–732, 2017.
[25] R. Vadivel, R. Suresh, P. Hammachukiattikul, B. Unyong, and N. Gunasekaran, "Event-triggered L_2–L_∞ filtering for network-based neutral systems with time-varying delays via T-S fuzzy approach," *IEEE Access*, vol. 9, pp. 145133–145147, 2021.
[26] R. Vadivel, P. Hammachukiattikul, G. Rajchakit, M. Syed Ali, and B. Unyong, "Finite-time event-triggered approach for recurrent neural networks with leakage term and its application," *Mathematics and Computers in Simulation*, vol. 182, pp. 765–790, 2021.
[27] Y. Tang, H. Gao, W. Zhang, and J. Kurths, "Leader-following consensus of a class of stochastic delayed multi-agent systems with partial mixed impulses," *Automatica*, vol. 53, pp. 346–354, 2015.
[28] L. Li, C. Li, and H. Li, "An analysis and design for time-varying structures dynamical networks via state constraint impulsive control," *International Journal of Control*, pp. 1–23, 2018.
[29] Y. Meng, Y. W. Wang, and J. W. Xiao, "Robust synchronization of impulsively-coupled complex switched networks with parametric uncertainties and time-varying delays," *Nonlinear Analysis: Real World Applications*, vol. 11, no. 4, pp. 3008–3020, 2010.
[30] C. Yi, C. Xu, J. Feng, J. Wang, and Y. Zhao, "Leading-following consensus for multi-agent systems with event-triggered delayed impulsive control," *IEEE Access*, vol. 7, pp. 136419–136427, 2019.
[31] W. Chen, W. Yang, and X. Lu, "Impulsive observer-based stabilisation of uncertain linear systems," *IET Control Theory & Applications*, vol. 8, no. 3, pp. 149–159, 2014.
[32] T. M. Guerra, H. Kerkeni, J. Lauber, and L. Vermeiren, "An e function for discrete T–S models: observer design," *IEEE Transactions on Fuzzy Systems*, vol. 20, no. 1, pp. 187–192, 2012.
[33] T. Raff and F. Allgower, "Observers with impulsive dynamical behavior for linear and nonlinear continuous-time systems," in *Proceedings of the 2007 46th IEEE conference on decision and control*, pp. 4287–4292, IEEE, New Orleans, LA, USA, 12-14 December 2007.